ON THE CLEAVAGE FRACTURE STRENGTH OF A BAINITIC MICROSTRUCTURE

H.Kotilainen *

The cleavage fracture strength of a bainitic steel has been found to consist of the Griffith stress, internal resistance of the crystal, strain hardening and of a probability term. The Griffith stress, applying the surface energy of pure ferrite (14 Jm^{-2}), gives a lower bound estimate for the cleavage fracture strength. The internal resistance of the crystal and the strain hardening term take the microstructure into account. Strain hardening is required to sustain a sufficient stress condition in the case of crack tip yielding and blunting. The maximum crack tip stress without strain hardening is thought to be the true microscopical cleavage fracture strength.

INTRODUCTION

Estimates of the cleavage fracture strength are mostly based on the Petch and Griffith formulae and therefore a $d^{-1/2}$ type of dependence on the grain size d has been presented. However, more current studies by Wobst and Aurich (1) and Curry (2) predict a $d^{-1/4}$ type of dependence. In the case of a complex microstructure as in weldments and in martensitic and bainitic microstructures it is not clear which is the fracture controlling grain size. There is fairly sound evidence that in bainite the fracture is controlled by the bainite packet, but not by individual laths nor by the prior austenite grain size (Brozzo et. al (3), Kotilainen and Törrönen, (4)). Also the effect of cold work in increasing the dislocation density and the cleavage fracture strength has been studied (1,5).

The importance of the dislocation density and small precipitates stabilizing the dislocation substructure on the fracture toughness has been considered (4, 6). Hence it is quite evident that the same factors which govern the yield strength also have an influence on the cleavage fracture strength including the packet size (Norström and Vingsbo (8)) and the lath width (Naylor (7)). Also a temperature dependent cleavage fracture strength has been postulated for a martensitic structure (8).

The mechanism of the initiation of a cleavage fracture has not been thoroughly investigated. A propagation controlled mechanism with existing stable microcracks has been postulated (3,6) but according to Curry (9) it seems not to be very likely, and rather a dislocation mechanism must operate.

*Imatran Voima, Electrical Laboratory, Viikintie 3, 00520 Helsinki 52, Finland

EXPERIMENTAL AND RESULTS

The material studied was a bainitic Cr-Mo-V alloyed steel with 0.16% C, 2.8% Cr, 0.6% Mo and 0.3% V. The heat treatment was a quench and temper, simulating the cooling of a thick plate. Three different heat treatments 940°C/5 h/600°C/20 h (M), 980°C/6 h/670°C/20 h (T) and 980°C/6 h760°C/20 h (K) were used. The prior austenite grain size is divided into packet bundles, which are composed of parallel packets. The packets are the smallest units surrounded by high angle boundaries. The packet size is not dependent on the prior austenite grain size. The packets are further divided into parallel laths and/or cells. The size and distribution of the MC-type carbides are both strongly dependent on the heat treatment. The microstructural units are given in Table 1.

TABLE 1 - Microstructural Units for Conditions K, T and M

Unit	Heat treatment condition K	T	M
Prior austenite grain (μm)	110	115	50
Packet (mean) (μm)	3.0	3.0	3.0
Mean diameter of the MC-type carbide (nm)	43.3	14.2	5.5
Planar interparticle spacing (nm)	466	131	51
Mesh length of dislocation network (nm)	135	82	49
Dislocation density (x 10^{-10}cm^{-2})	2	6	16
Fracture facet (μm)	3.3	3.6	3.4

Tensile tests were performed in the temperature range 12-300 K. The yield strength was taken to be the lower yield strength value or the 0.2% proof strength. The results are given in Figure 1 for all three heat treatment conditions.

The strain hardening exponent was calculated using the tensile test results and it is given as a function of temperature in Fig. 2. Fig. 3 shows the results of the static Charpy V bend tests performed with the T and M conditions. The general yield load has been calculated using the expression (1).

$$F_{GY} = \frac{\sigma_Y}{S} \cdot 1{,}26 \cdot B(W-a)^2 \qquad (1)$$

The fracture toughness K_{IC} has been measured using 25 mm thick CT and 3-point bend specimens and one 75 mm thick specimen. Valid K_{IC} values were measured up to 185 K, and these values are denoted in Figure 4 with filled points. The K_{IC} versus temperature curve has been estimated between the temperatures 185 K and 260 K using the J-integral calculation method reported by Chell and Milne (11). All specimens up to 260 K showed a cleavage type fracture. The bimodal behaviour of the results will be discussed later.

The size of the fracture facet was measured from polished sections by means of scanning electron microscopy.

DISCUSSION

The results of the slow bend tests of Fig. 3 have been used to estimate the cleavage fracture strength applying the Green and Hundy solution Eq (2).

$$\sigma_k = \sigma_Y (1 + \frac{\pi}{2} - \frac{w}{2}) \quad (2)$$

In Eq. (2) w = 45° is the notch flank angle. For the conditions T and M values of 2075 Nmm^{-2} and 2525 Nmm^{-2}, respectively, can be calculated assuming Tresca's yield criterion.

The maximum stress in front of a sharp crack can be calculated using the Rice and Rosengren (12) solution for a strain hardening material. Performing the calculation using the data of Fig. 2 the maximum crack tip stress shown in Fig. 5. can be obtained.

Taking the lowest value of σ_y^{max} not influenced by the strain hardening, values of 2500 Nmm^{-2}, 3050 Nmm^{-2} and 3700 Nmm^{-2} for the heat treatment conditions K, T and M can be obtained, respectively. It is fairly obvious that these values are closely related to the mesh length of the dislocation network (L_m) or dislocation density (ρ_d) L_m = const.x $\rho_d^{-1/2}$, which also determines the value of the yield strength. This is demonstrated in Fig. 6.

The stress σ_f assumed to be equal to σ_y^{max} can be attained without strain hardening by stress concentration only. The value of σ_f is, however, much higher than the value of σ_k calculated for the blunt notch case. This difference could be accounted for by the higher sampling capability of the blunt notch and strain hardening.The highly stressed volume ahead a blunt notch is larger than in front of a crack. Therefore the probability of finding the weakest link is higher in the case of a blunt notch than in the case of a crack.

This idea has been demonstrated by Kaechele and Tetelman (13) by Eq. (3).

$$\sigma_f = \sigma_{fc} \left(\frac{V_t}{V_c} \right)^{1/N} \quad (3)$$

N is a constant with a theoretical value of 9 according to (13).

The validity of Eq (3) can checked for blunt notch bend specimens as well as for tensile specimens. The minimum value of the true fracture strength R_f for the different heat treatment conditions are 995 Nmm^{-2} (K), 1220 Nmm^{-2} (T) and 1505 Nmm^{-2} (M). This value is the fracture strength without excessive strain hardening and could be compared to the σ_f value of a cracked specimen.

Assuming that the size of the fracture process zone is equal to the plane strain plastic zone size r_Y, the volume V_c can be calculated as a first approximation according to Eq (4)

$$V_C = {}^1/_4 \pi r_Y^2 B \qquad (4)$$

where B is the thickness of the specimen (25 mm). The volume of tensile specimen can be considered as the volume inside the gauge length. The tensile tests have been performed using ø 5mm specimens with 50 mm gauge length.

Using the fracture toughness data of Figs. 1 and 4, the relation of σ_f to the minimum value of R_f and applying the Eqs. (3) and (4) the value of N for the conditions T and K can be calculated as 11.5 and 9.1, respectively. These values do not differ very much from the theoretical values in spite of the rough estimates of the process volume. Therefore it can be concluded that the difference between σ_f and the minimum of the R_f could be due to the different sizes of the stressed volumes.

The same calculation can be performed also for the blunt notch specimen in which the plastic zone size R can be expressed according to Tetelman and McEvily (14) Eq (5).

$$R = \rho \left[\exp\left(\frac{\sigma_k}{\sigma_Y} - 1\right) - 1 \right] \qquad (5)$$

This calculation results in values of 11.3 and 11.5 for N for the conditions T and M, respectively. Again a close agreement can be found between the theoretical value and the figures given above for the tensile test case.

The approximate calculations show that the cleavage fracture strength depends among other things on the size of the stressed volume i.e. on the probability of finding a critical weak point.

The lower bound cleavage fracture strength σ_{fG} can be estimated applying the Griffith formula Eq. (6)

$$\sigma_{fG} = \left(\frac{2E\gamma}{(1-\nu^2)\pi a} \right)^{1/2} \qquad (6)$$

Using the effective surface energy 14 Jm^{-2} (9, 15) which has been found applicable for ferrite, and the fracture facet size as a crack length, a value of 1060 Nmm^{-2} can be calculated for all three heat treatment conditions. Considering the actual values of the yield strengths it is quite clear that the fracture strength according to Eq. (6) cannot be a true cleavage fracture strength. Eq. (6) assumes only that a microcrack of given size begins to propagate through a crystal the resistance of which is determined by the surface energy only. It has been shown, however, that the cleavage fracture strength increases with increasing amount of cold work i.e. with increasing dislocation density (1,5). In pure zinc Messmer et al (16) have found that the increase of dislocation density even lowers the surface energy.

In summary, the cleavage fracture strength can be broken down into separate parts. First we could have stress for micro-

crack propagation in pure ferrite σ_{fG} i.e. the Griffith stress with the surface energy of 14 Jm^{-2} (15). To this stress we should add the term which includes the internal resistance of the crystal to the crack propagation (σ_o), which depends on the microstructural constituents like dislocation density, carbide distribution etc. As a first approximation we could assume that σ_o is equal to the temperature independent part of the yield strength. The third term depends on the strain hardening capability in the stressed volume and possibly on the probability of finding the weakest link.

Now the cleavage fracture strength σ_{fc} can be expressed as

$$\sigma_{fc} = \sigma_{fG} + \sigma_o + \sigma_p \qquad (7)$$

Applying this Eq. (7) for the material considered the following figures can be obtained (Table 2).

Table 2 Calculated Cleavage Fracture Strength for Heat Treatment Conditions K, T and M.

Cond.	σ_{fG} (Nmm^{-2})	σ_o [1] (Nmm^{-2})	$\sigma_{fc}-\sigma_p$ (Nmm^{-2})
K	1060	285	1345
T	1060	500	1560
M	1060	905	1965

1) Kotilainen et.al. (17)

The value $\sigma_{fc} - \sigma_p$ can be considered as the cleavage fracture strength of an unnotched tensile specimen without strain hardening. The value of σ_p can be estimated considering the blunt notch values given before and the maximum value σ_p^{max} in case of cracked specimen i.e. $\sigma_y^{max} - (\sigma_{fc}-\sigma_p)$.

Table 3 Estimated Values of σ_p (Nmm^{-2})

Cond.	Notch		Crack	
	σ_{fc}	σ_p	σ_y^{max}	σ_p^{max}
K	-	-	2500	1155
T	2075	515	3050	1490
M	2525	560	3700	1735

The values of σ_p according to Table 3 are quite large and therefore it must be understood that σ_p sustains the sufficient stress gradient at the crack tip. It must be also remembered that σ_p^{max} is the highest theoretical value and not necessary the true strain hardening which is required to exceed the cleavage fracture strength.

The high value of σ_p^{max} implies that in the case of a cracked specimen with no strain hardening a very high stress must be attained before fracture commences. The maximum stress at the tip of a crack with no strain hardening which cause fracture can be considered as a true microscopical cleavage fracture strength.

In this case the fracture is controlled by the mechanism. This means that when the first slip occurs the sufficient conditions for fracture are obtained.

At higher temperatures, at which yielding and strain hardening occur, the first slip is no longer sufficient condition for fracture, but rather the formation of a microcracks. The microcracks together with strain hardening produce a sufficient increase of the stress in front of the main crack tip, which is blunted due to the initial yielding. Now also the probability of finding a critical microcrack and the stressed volume must be considered.

The model described above implies also that at least in a certain temperature range stable microcracks are formed in bainite in spite of some contradictory results (9). On the other hand it is not quite clear how in a microstructure with high dislocation density and high amount of dislocation locking carbides, a repetitive dislocation glide mechanism could work and produce a sufficient pile-up to create a crack.

It is thought that there is no abrupt change in the fracture controlling mechanism. Depending on the yielding characteristics a rather smooth transition from the mechanisms controlled fracture to microcrack and strain hardening controlled fracture is assumed. In a material having a particular microstructure these two mechanisms can be competetive processes and the probability term determines which mechanism is operative in the transition region. This competition is thought to be the reason for the bimodal behavior of the fracture toughness of the condition T in the temperature range of 140 K to 200 K in Fig. 4.

SYMBOLS USED

$2a$ = crack on notch length
B = specimen thickness
E = Young's modulus
F_{GY} = force at general yield
K_{IC} = plane strain fracture toughness
r_Y = size of the plastic zone of a cracked specimen
R = " " notched "
$R_{po.2}$ = proof strength
R_f = true fracture strength
S = span width
V_c = volume of the stressed zone in cracked specimen
V_t = " " tensile specimen
W = specimen width
γ = effective surface energy of iron
ρ = notch root radius
σ_Y = yield strength
σ_k = peak stress at a root of notch
σ_f = fracture stress
σ_{fc} = cleavage fracture stress
σ_{fG} = Griffith stress
σ_{max} = peak stress at the tip of crack
σ_y = internal resistance of a crystal to cleavage
σ_o = critical stress needed to exceed the true microscopical cleavage fracture strength
σ_p

REFERENCES

1. Wobst, K. and Aurich, D., 1976,; DVM 8. Sitzung des Arbeitskreises Bruchvorgänge, Köln, DVM, Berlin, 145

2. Curry, D.A., 1979, Fortschr.-Ber.VDI-Z, 18, 6, 214

3. Brozzo, P., Buzzichelli, G., Mascanzoni, A., Mirabile, M., 1977, Met. Sci., 11, 123

4. Kotilainen, H., Törrönen, K., 1977, Fracture 1977, Vol. 2, Ed. D.M.R.Taplin, Univ. Waterloo Press, 57

5. Groom, J.D.G., Knott, J.F., 1975, Met. Sci., 9, 390

6. Kotilainen, H., 1980, Fatigue and Fracture, Ed. J.Radon, Pergamon Press., Oxford, 217

7. Naylor, J.P., 1979, Met. Trans., 10A, 861

8. Norström, L.-Å., Vingsbo, O., 1979, Met. Sci, 13, 677

9. Curry, D.A., 1981, CEGB Note DR/L/N 154/80

10. Törrönen, K., 1979, Tech. Res. Centre of Finland, Publ. 22

11. Chell, G.G., Milne, I., 1976, Mat. Sci. and Eng., 22, 249

12. Rice, J.R., Rosengren, G.F., 1968, J. Mech. Phys. Solids, 16, 1

13. Kaechele, L.E., Tetelman, A.S., 1969, Acta Met. 17, 463

14. Tetelman, A.S., McEvily Jr., A.J., 1967, Fracture of Structural Materials, John Wiley, New York

15. Knott, J.F., 1977, Fracture 1977, Vol. 1, Ed. D.M.R.Taplin, Univ. Waterloo Press, 61

16. Messmer, C., Bilello, J.C., Dew-Hughes, D., 1981, Met. Sci. 15, 79

17. Kotilainen, H., Törrönen, K., Nenonen, P., 1979, Proc. 5th Int. Conf. on Strength of Metals and Alloys, Vol. 2, Eds. P. Haasen, V. Gerold & G. Kostorz, Pergamon Press, Oxford, 1431

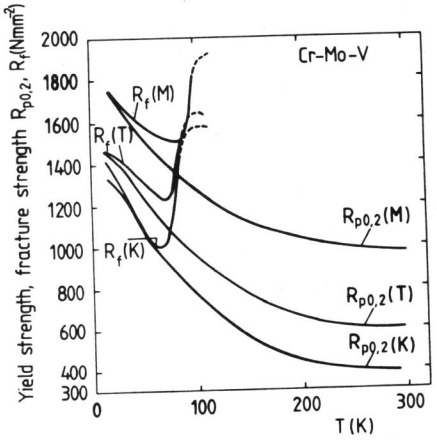

Figure 1. Fracture and proof strength

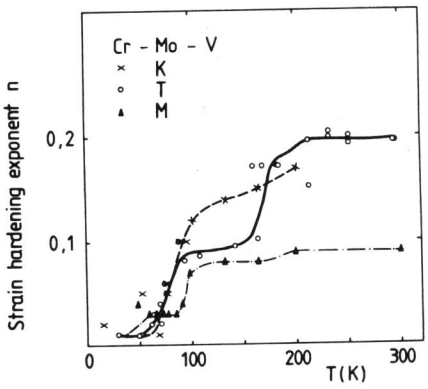

Figure 2. Strain hardening exponent

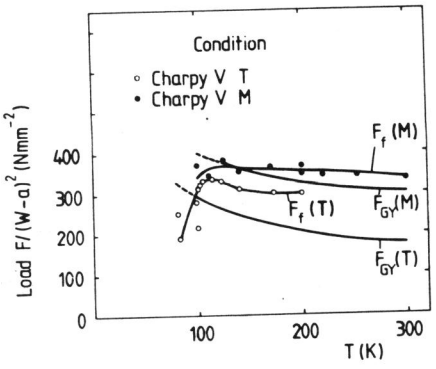

Figure 3. Slow bend test results

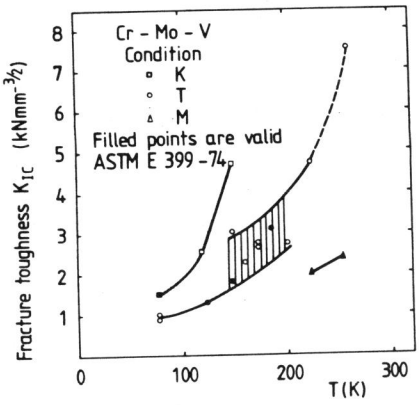

Figure 4. Fracture toughness

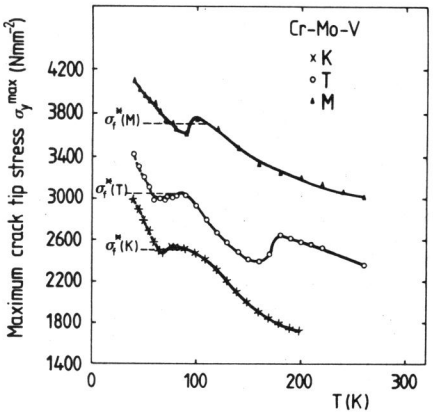

Figure 5. Maximum crack tip stress

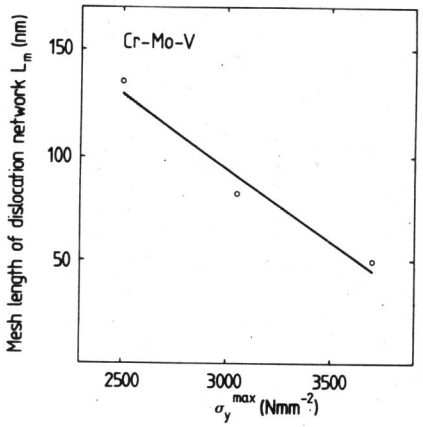

Figure 6. Crack tip stress as a function of dislocation mesh length